

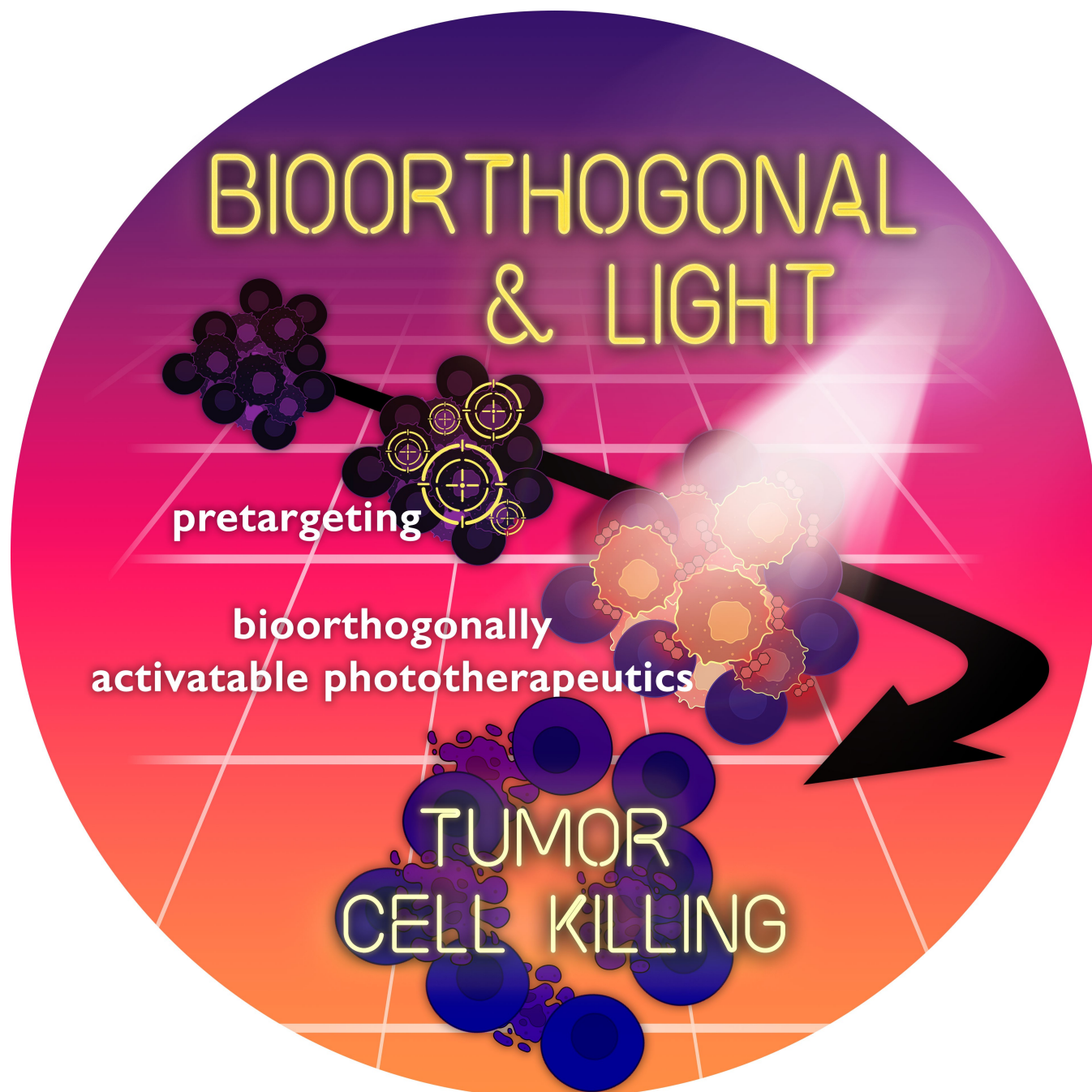
Photochemistry

How to cite:

doi.org/10.1002/anie.202303198

# Bioorthogonally Assisted Phototherapy: Recent Advances and Prospects

Eszter Kozma, Márton Bojtár, and Péter Kele\*



**Abstract:** Photoresponsive materials offer excellent spatiotemporal control over biological processes and the emerging phototherapeutic methods are expected to have significant effects on targeted cancer therapies. Recent examples show that combination of photoactivatable approaches with bioorthogonal chemistry enhances the precision of targeted phototherapies and profound implications are foreseen particularly in the treatment of disperse/diffuse tumors. The extra level of on-target selectivity and improved spatial/temporal control considerably intensified related bioorthogonally assisted phototherapy research. The anticipated growth of further developments in the field justifies the timeliness of a brief summary of the state of the art.

## 1. Introduction

Lately, enormous effort has been undertaken to exploit light as an external trigger in chemical and biological sciences. These efforts have brought remarkable advances in light-related techniques allowing them to grow from simple means of observation to a precision tool in a wide range of applications.<sup>[1–3]</sup> The use of light as an external trigger has also resulted in the emergence of several phototherapeutic approaches, which are foreseen to have profound implications on targeted therapies.<sup>[4–6]</sup> These photoactivated therapies offer excellent localization-precision in case of localized solid tumors. Selective treatment of dispersed/diffuse tumor cells, especially when spread to several different locations in the body, is however, an enormous challenge, which highlights the need for advanced targeting mechanisms.<sup>[7,8]</sup> Toward the ultimate goal of reaching selectivity for cancer cells, the combination of light with bioorthogonal targeting is notable. Recently, an increasing number of examples was reported on bioorthogonalized photoresponsive species where the bioorthogonal step facilitates selective targeting of a photoresponsive unit to the vicinity of cancer cells. In certain instances, however, the role of the bioorthogonal reaction goes way beyond this and has an added feature of activating the photoresponsivity upon ligation allowing to gain even higher spatiotemporal control over light-triggered processes. Since very thorough, excellent summaries on the particular phototherapeutic approaches<sup>[9–12]</sup> as well as on bioorthogonal tools<sup>[13–15]</sup> were published recently, we discuss these just briefly and focus on examples where photoresponsivity is modulated in the bioorthogonal step.

## 2. Phototherapeutic modalities and bioorthogonality

### 2.1. Making light toxic

Phototherapies rely on the use of photoactive molecules that respond variously to light irradiation. The particular modality of the phototherapeutic approach depends on the pathway these photoactive species undergo to release the excess energy of their respective excited states.

*Photodynamic therapy* (PDT) is a non-invasive form of light therapy that has played a significant role in dermatology for several decades and receiving increasing attention in gynecology and oncology related treatments.<sup>[10,16–20]</sup> In PDT, light irradiation converts a photosensitizer (PS) from a singlet ground state ( $S_0$ ) to an excited triplet state ( $T_1$ ) via intersystem crossing from an excited singlet state. In  $T_1$ , the PS can undergo electron transfer (type I) or energy transfer (type II) processes leading to the production of various reactive oxygen species (ROS) (Figure 1).

These reactive species (radical anions  $O_2^{\bullet-}$ ,  $HO^{\bullet}$  or singlet oxygen,  $^1O_2$ ) cause photodamage of biological molecules resulting in necrosis and/or apoptosis of light-exposed diseased cells/tissues.<sup>[16,21]</sup> Amongst phototherapeutic modalities PDT is the most advanced that has already reached clinical application.<sup>[10]</sup> Its successful translation to medicine has also resulted the availability of advanced light delivery technology that can be directly applied to further phototherapies.

Photothermal transduction agents (PTTAs) convert photonic energy into thermal energy through non-radiative decay.<sup>[22]</sup> This feature is harvested in *photothermal therapy* (PTT),<sup>[10,23]</sup> *photoacoustic imaging* (PAI) and *photoacoustic therapy* (PAT).<sup>[24]</sup> Following excitation of a PTTA by light at wavelengths corresponding to the resonant energy of the PTTA, its conduction-band electrons start to oscillate synchronously resulting in the production of heat leading to substantially elevated local temperatures sufficient to cause cellular damage and subsequent tumor regression.<sup>[23]</sup> In photoacoustic applications the temperature increase is followed by a pressure rise through instant thermoelastic expansion.<sup>[25,26]</sup> The pressure induced acoustic wave is propagated through the tissue and detected as a photoacoustic signal. PAT is utilizing the enhanced photoacoustic wave generated by pulsed laser irradiation accumulated in the tumor tissue.<sup>[27]</sup> The mechanic damage to the target cells is free from side effects of chemotherapeutics and not restricted to oxygen perfused tumors such as PDT.

[\*] E. Kozma, M. Bojtár, P. Kele

Chemical Biology Research Group, Institute of Organic Chemistry, Research Centre for Natural Sciences, Eötvös Loránd Research Network, Magyar tudósok krt. 2, 1117 Budapest (Hungary)  
E-mail: kele.peter@ttk.hu

© 2023 The Authors. Angewandte Chemie International Edition published by Wiley-VCH GmbH. This is an open access article under the terms of the Creative Commons Attribution License, which permits use, distribution and reproduction in any medium, provided the original work is properly cited.

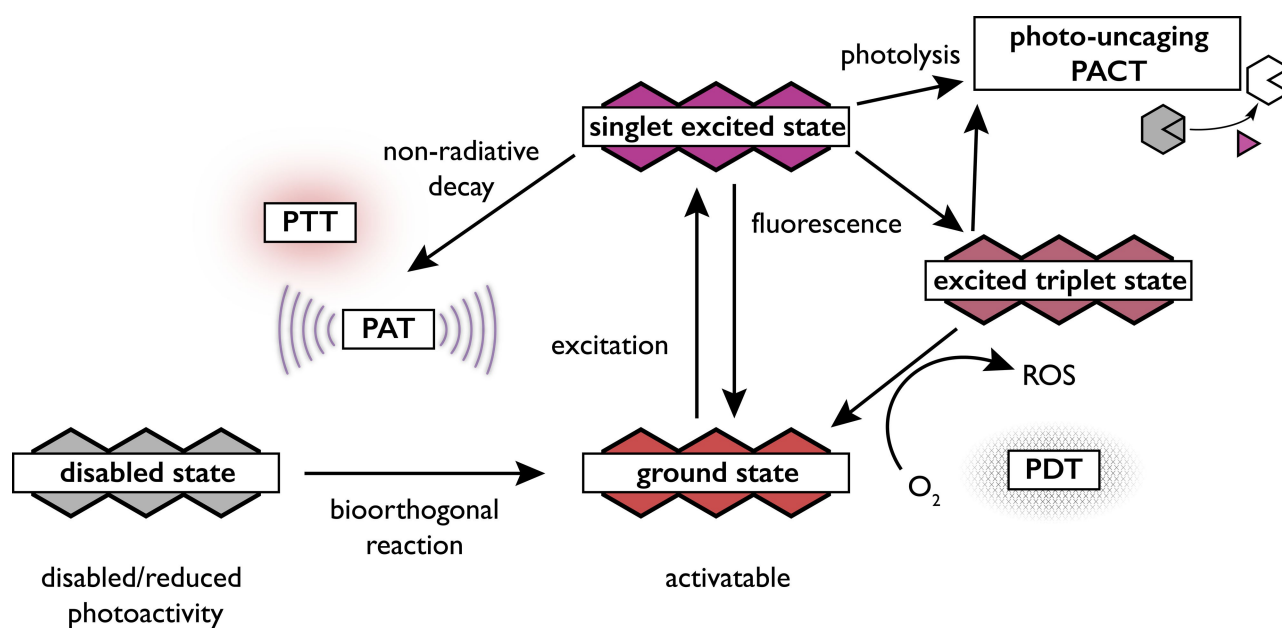


**Figure 1.** Schematic representation of bioorthogonally assisted phototherapies (PDT: photodynamic therapy, PACT: photoactivated chemotherapy, PTT: photothermal therapy, PAT: photoacoustic therapy).

*Photoactivated chemotherapy (PACT)* combines some of the beneficial effects of external radiation therapy and internal chemotherapy of cytotoxic drugs. Masking the activity of chemotherapeutic drugs with photolabile protecting groups (PPGs) is a promising solution for oxygen-independent phototherapy.<sup>[5,11,28]</sup> Light-induced removal of

these photolabile moieties from the prodrugs by light irradiation leads to liberation of the cargo thus the activity of the caged substrate restores.<sup>[12,29]</sup> Clinical translation of PACT, however, is still hindered by the lack of suitably hydrophilic PPGs activatable in the biologically benign red or near-infrared (NIR) range, although considerable advan-



*Eszter Kozma graduated as a pharmacist at University of Szeged, Hungary. She spent a year at the National Institutes of Health (USA) under the supervision of Prof. Kenneth A. Jacobson. During her Ph.D., she was a visiting fellow at the European Molecular Biology Laboratory (Heidelberg, Germany) and Institut de Biologie del École Normale Supérieure (Paris, France). She obtained her Ph.D. at Eötvös Loránd University, Hungary in 2018. Since 2022, she is a research associate in Dr. Péter Kele's lab studying neuron-astrocyte interactions using photocaged neuromodulators.*



*Márton Bojtár earned his Ph.D. degree at the University of Technology and Economics, Budapest in 2017. Since then, he mostly worked as a research associate in Péter Kele's lab. In 2022, he spent a semester at Evan W. Miller at the University of California, Berkeley as a Fulbright Fellow. His main research area is the development, functionalization and application of photocages and photo-responsive materials.*



*Péter Kele obtained his Ph.D. from the University of Miami in 2002 under the supervision of Prof. Roger M. Leblanc. He then received an Alexander von Humboldt Fellowship to further his knowledge of fluorescent probes at the University of Regensburg under the supervision of Otto S. Wolfbeis. Currently, he is leading the Chemical Biology Research Group at the Research Centre for Natural Sciences, Budapest, Hungary focusing on the development of bioorthogonally applicable fluorogenic probes and exploring novel ideas in photolabile protecting group activation mechanisms.*

ces have been made recently, for example by the development of two-photon photocages.<sup>[11,30,31]</sup>

## 2.2. The bioorthogonal “click-bait”

The Nobel-prize winning idea of using non-native, highly energetic, yet non-interfering, i.e., chemically and biologically inert functions to achieve biocompatible, selective ligation methods has revolutionized the field of chemical biology.<sup>[32]</sup> Within the last two decades, several reports have demonstrated how bioorthogonal chemistry can assist selective targeting of probes or drugs even in vivo.<sup>[13–15,33]</sup> Unlike conventional, synthetic biology-based approaches that allow selective tagging or targeting of proteins, bioorthogonal methods also enable selective modification of biomolecules e.g., nucleic acids, lipids, sugars, small metabolites, ligands etc. that are not directly encoded in the genome.<sup>[34–36]</sup> In the context of phototherapies, bioorthogonal chemistry tools are mainly applied for the selective delivery of a photoresponsive unit to the target area e.g., in combination with antibodies, small molecular ligands or metabolic engineering. Some improvements, however, have gone beyond this and furnished the bioorthogonal step with the extra feature of modulating the photoresponsivity. Such on-site activation of the light responsive elements is based on the changes in the photoresponsivity at a certain wavelength of light as a result of conformational, electronic etc. changes triggered by the bioorthogonal ligation step. The concept is projected to allow pre-targeting based approaches, where the tumor cells are first targeted with a specific targeting moiety (e.g., antibody) tagged with a bioorthogonal handle, then, following accumulation, a quenched photoresponsive element, bearing the complementary bioorthogonal motif is administered.

## 3. Combining phototherapeutic modalities with bioorthogonality

### 3.1. Bioorthogonally aided photosensitizers of reactive oxygen species

The extensive research on bioorthogonally applicable fluorogenic probes have pointed out that similarly to fluorescence, photoresponsivity of some particular cores can also be transiently quenched by certain bioorthogonal functions i.e., the azide or tetrazine motifs.<sup>[37–42]</sup> Once these bioorthogonal motifs participated in a bioorthogonal ligation reaction (e.g., with a functionalized pre-targeting vehicle), the photoresponsive unit becomes active again. Besides the reinstated phototherapeutic modality, fluorescence of such systems also increases considerably, enabling parallel imaging of the probes as well.

Boron dipyrromethene (BODIPY) is widely used as a fluorescent core and as a PS with enhanced triplet state quantum yield.<sup>[43]</sup> Based on BODIPY-tetrazine fluorogens,<sup>[39]</sup> Vázquez and co-workers prepared BODIPY-tetra-

zine PSs that can be activated via inverse electron-demand Diels–Alder (IEDDA) reaction between a 1,2,4,5-tetrazine and norbornene as the dienophile.<sup>[44]</sup> The authors prepared an iodinated BODIPY-derivative (**1**) with a directly conjugated tetrazine unit (Figure 2a). The tetrazine quenched the PS through an excited state energy transfer process from the BODIPY to the tetrazine unit. This results in an efficient  $T_1 \rightarrow S_0$  transition that proceeds through the tetrazine via a nonradiative decay channel with markedly decreased ROS production. Once the IEDDA reaction took place, this relaxation pathway is no longer available, which leads to increased ROS sensitization properties (i.e.,  $\Phi_{\Delta} = 0.22$  for the tetrazine vs. 0.51 for the pyridazine). In case of the pyridazine product, a ten-fold decrease in the  $IC_{50}$  value was observed upon light irradiation ( $IC_{50}$  1.92  $\mu\text{M}$  (tetrazine) vs 0.212  $\mu\text{M}$  (pyridazine)), enabling PDT on HeLa cells with metabolically bioorthogonalized DNA using 5-vinyl-2'-deoxyuridine (VdU) (Figure 2a). Active targeting of overexpressed receptors (e.g., with aptamers, antibodies peptides or folates) enable precise delivery of PSs to tumor sites.<sup>[45]</sup> Nevertheless, these conjugates are moderately taken up by normal cells as most cancer-associated receptors are not solely expressed on cancer cells. To circumvent this problem, dual receptor targeting was applied by Ng et al.<sup>[46]</sup> In their recent work, a biotinylated BODIPY-tetrazine derivative (**2**) was internalized concurrently with a BCN-conju-

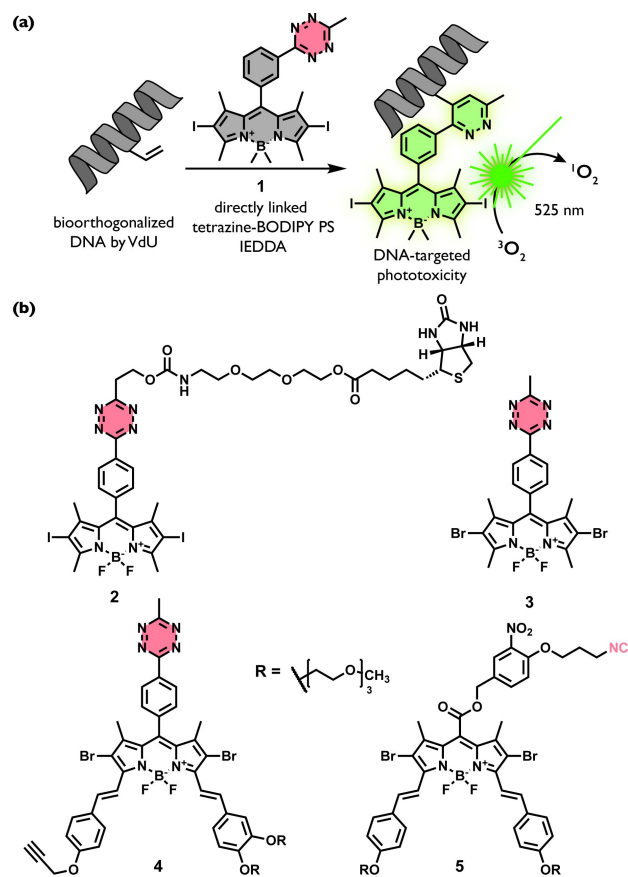


**Figure 2.** Schematic illustration of mechanism of action (a) and structure (b) of BODIPY-based activatable photosensitizers.

gated epidermal growth factor receptor (EGFR)-targeting cyclic peptide. Only in cancer cells overexpressing both receptors (e.g., A549 human lung carcinoma cells) the two compounds underwent an IEDDA reaction leading to increased photodynamic activity of the BODIPY core and nearly full ablation of cancer cells after light irradiation. The same group implemented an active targeting approach using biotin receptor positive cancer cells (HeLa) and a *trans*-cyclooctene (TCO)-conjugated biotin as a pretargeting element for subsequent reaction with their BODIPY-tetrazine, **3** PS.<sup>[47]</sup> Upon irradiation with  $\lambda > 515$  nm light, high cytotoxicity was observed with an  $IC_{50}$  value of 170 nM, while no appreciable toxicity was detected in the dark. A derivative of **3** with extended  $\pi$ -conjugation system was also prepared. This distyryl boron dipyrromethene (DSBDP)-based PS (**4**) was also equipped with two triethylene glycol side-chains to enhance hydrophilicity.<sup>[48]</sup> Although the sensitizing potential of this red-shifted compound ( $\lambda_{abs} = 610$  nm) was not significantly quenched by the tetrazine unit, pretargeting A431 cells with EGFR substrate TCO-GE11 peptide conjugate, with subsequent irradiation resulted in increased cytotoxicity compared to non-pretargeted cells, which was attributed to the enhanced permeability of the PS. This latter example also highlights the limitation of tetrazine-based modulation of photoresponsivity in case of frames with absorption over 550 nm, as observed by us and others in case of fluorogenic probes.<sup>[40,41]</sup> To address the wavelength limitation, Xiong and co-workers made a  $\pi$ -extended BODIPY scaffold with chemically quenched photoresponsivity in its bioorthogonal motif containing ester form (**5**).<sup>[49]</sup> The ester was found to readily degrade to a photoactive carboxylate form through the self-immolation process triggered by the reaction of a novel bioorthogonal motif, isonitrile with a tetrazine. They have demonstrated

the viability of this design by reinstating the ROS generating activity of their isonitrile-PS upon reaction with tetrazine-tagged cancer cells.

Further attempts to hijack the limitations of tetrazine-based quenching triggered the exploration of various alternative mechanisms. Rhodamine derivatives with chalcogen replacement in the 10-position (such as selenorhodamines—SeR) are ideal candidates for PDT with good water-solubility, high absorption coefficient and singlet oxygen quantum yield.<sup>[50]</sup> Spirocyclization of rhodamine derivatives is a well-known feature that was exploited in the design of fluorogenic probes, fluorescent chemosensors and activatable PSs.<sup>[40,51,52]</sup> These derivatives are colorless in their spirocyclic forms thus cannot generate ROS. Liu and co-workers took advantage of the electronic effects of certain substituents that shift the equilibrium of the spirocyclization process. Their design included a  $\pi$ -extended, red-absorbing Se-rhodamine (**SeR-azide**, **6**) carrying a masked amine in the form of an azide. The electronic properties of the azide locked the SeR in its colorless form (Figure 3a).<sup>[53]</sup> When the azide was unmasked to its respective amino derivative in a Staudinger reaction with triphenylphosphine derivative (TPP), the photoactive, open form became dominant. Such bioorthogonal reaction-based activation of the sensitizing property allowed efficient  $^1O_2$  production ( $\Phi_{\Delta} = 0.35$ ) upon red light (610 nm) illumination. Such use of **SeR-azide** was demonstrated in TPP- and light-induced apoptotic cell death of HeLa cells.

Fluorogens with aggregation-induced emission (AIEgens) represent another approach of activatable PSs.<sup>[54,55]</sup> AIEgens are characterized by their virtually zero emission in their molecularly dissolved state but emit strong fluorescence when aggregated due to suppression of non-radiative relaxation pathways by restricted rotation. Besides

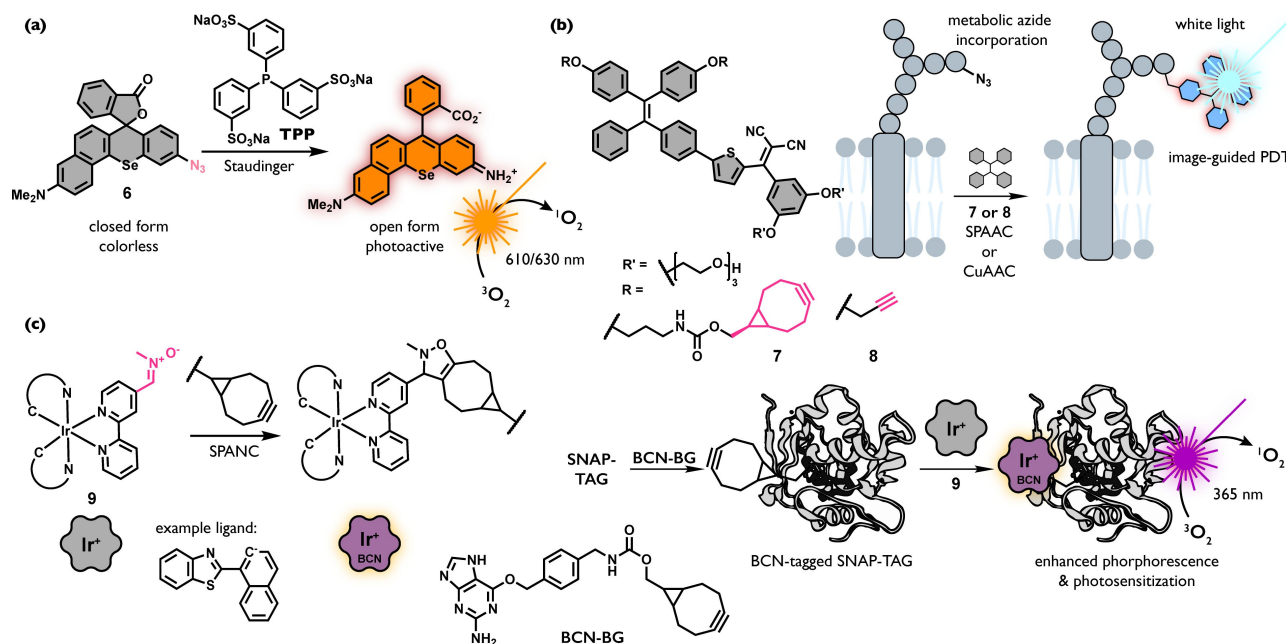


**Figure 3.** Activatable photosensitizers based on a) selenorhodamine, b) aggregation-induced emission and c) iridium(II)-polypyridine complexes.

their fluorogenic potential certain AIEgens are also prone to ROS generation under light illumination. Prompted by these, the Liu group developed tetraphenylethylene derived PS precursors (TPET, TPETSAI) with appending cyclooctyne, (BCN) (**7**) or terminal alkyne (**8**) function, respectively.<sup>[56,57]</sup> Cancer cell lines (4T1 or HeLa) were metabolically tagged with azide functions in their surface glycans using azide-tagged unnatural sugars Ac<sub>4</sub>ManNAz or AzAcSA, respectively. Upon treatment of the azide tagged cells with **TPET-BCN** (**7**) or **TPETSAI-alkyne** (**8**) the bioorthogonal reaction (strain-promoted azide-alkyne cycloaddition—SPAAC or copper-catalyzed azide alkyne cycloaddition—CuAAC, respectively) brought the probes into close proximity, leading aggregation of the probes to result in increased photoresponsivity both in terms of fluorescence and ROS sensitizing ability (Figure 3b).

Transition metal complexes have long-lived triplet states that render them efficient <sup>1</sup>O<sub>2</sub> PSs.<sup>[58,59]</sup> Lo and co-workers explored the modulation of the sensitizing ability of iridium(III) polypyridine complexes (**9**) by an appended nitron bioorthogonal motif.<sup>[60]</sup> The nitron participates in strain promoted alkyne-nitron cycloaddition (SPANC) with a SNAP-tag substrate BCN-benzylguanine (BCN-BG). The authors expressed SNAP-tagged fused endoplasmic reticulum (ER)-targeting protein and cytoplasm-enriched SNAP-tag in Chinese hamster ovary (CHO)-K1 cells. Following treatment of the cells with BCN-BG then with nitron-quenched complexes the authors reported enhanced phototoxicity (IC<sub>50</sub> = 0.34 μM at 365 nm, 30 min) compared to non-pretargeted transfected (IC<sub>50</sub> = 20.9 μM) or pretargeted non-transfected cells (IC<sub>50</sub> = 19.5 μM) (Figure 3c).

Nanomaterials have been widely adopted to several light-assisted therapeutic applications.<sup>[6,61,62]</sup> Their bioorthogonally controlled activation, however, requires different approaches. Tumor-targeting nanoparticles are generally prepared by adjusting physical properties or by conjugation of bioactive molecules. However, the limited number of cellular receptors and heterogeneity of tumor tissues limit their applications. Delivery of the bioorthogonal reaction partner to cancer cells via enhanced permeation and retention (EPR) effect is an effective method as described by Kim et al. in 2014.<sup>[63]</sup> EPR effect is responsible for the accumulation of nanoparticles (NP) into tumor tissues through passive or active transport.<sup>[64–67]</sup> Yang et al. took advantage of EPR effect when intravenously administered Ac<sub>4</sub>ManNAz encapsulated in poly(ethylene glycol)-block-poly lactide nanoparticles (Az-NP) into A549 tumor-bearing mice to introduce site-specific azide-groups onto the surface of tumor cells.<sup>[68]</sup> They performed a second intravenous injection using acid responsive nanoparticles (S-NPs) doped with dibenzocyclooctyne (DBCO) equipped chlorin e6 (Ce6-DBCO). The acidic microenvironment of the tumor site led to the disassembly of the NPs exposing DBCO-Ce6 that could then be anchored to the surface of tumor cells by SPAAC. Light irradiation resulted in tumor growth inhibition as guided by fluorescence and T2-weighted MR dual-modal imaging. Tumor selectivity can be further improved by bioorthogonal assembly of drug cargos.<sup>[69]</sup> In general, two nanoparticles bearing complementary bioorthogonal groups

are taken up by EPR and react at the tumor site further localizing the PDT effect. Yu et al. prepared a polymeric proteolysis targeting chimera (POLY-PROTAC) targeting bromodomain BRD4.<sup>[70]</sup> The authors assembled a tumor-localized drug cargo from DBCO-NP and azide-POLY-PROTAC-NP filled with PS pheophorbide A copolymer. Inside the MDA-MB-231 breast cancer tissue multiple triggers (extracellular matrix metalloprotease 2 enzyme, intracellular acidic pH and GSH) liberated PROTAC and PS (Figure 4). While PROTAC realized antitumoral bromodomain BRD4 proteolysis, laser irradiation at 671 nm generated PDT effect which resulted in significant tumor regression.

### 3.2. Bioorthogonally activated photothermal transduction agents

As far as we are aware, no example for bioorthogonal modulation of PTT activity is reported yet. However, there are a few examples to use bioorthogonal chemistry to deliver PTTAs more efficiently to cancer cells. Yao et al. developed a DBCO-modified nanocomposite system (DLQ/DZ) to deliver doxorubicin (DOX) and PTTA zinc phthalocyanine (ZnPc) for chemo-photothermal therapy.<sup>[71]</sup> Tumor cell surface was modified via intratumoral injection of Ac<sub>4</sub>ManNAz into MCF-7 tumor bearing mice. Subsequent i.v. injection of DLQ/DZ allowed SPAAC reaction leading to enhanced tumor-specific distribution (4.6× increase) resulting in a 96.1% tumor inhibition rate. Huang and co-workers combined PTT with NIR-IIa (1000–1700 nm) imaging in a theranostic platform.<sup>[72]</sup> The authors synthesized a semi-conducting polymer nanoparticle PTTA (PSQNP) equipped with a DBCO bioorthogonal handle. Colorectal cancer cells CT26 were labelled with azide via metabolic glycoengineering and reacted with PSQNPs-DBCO resulting in 71.7% cell toxicity, however, with significant toxicity (45.8%) in the absence of light (1064 nm) as well. Cai and co-workers combined metabolic azide labeling with immune cell membrane recognition strategy for site-specific cancer localization (Figure 5).<sup>[73]</sup> They coated widely used PTTA indoc-

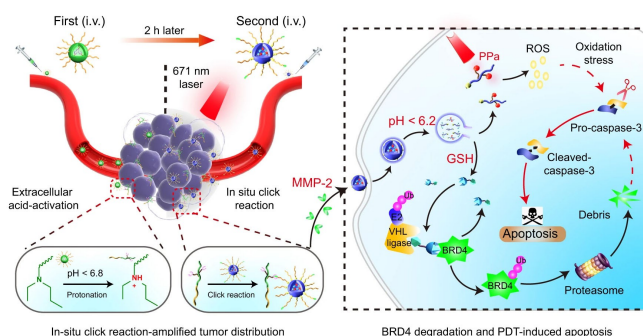


**Figure 4.** Schematic illustration of POLY-PROTAC nanoparticles for tumor-specific protein degradation and PDT (adapted from Ref. [70] with permission. Copyright © 2022, The Authors, Published by Springer Nature).

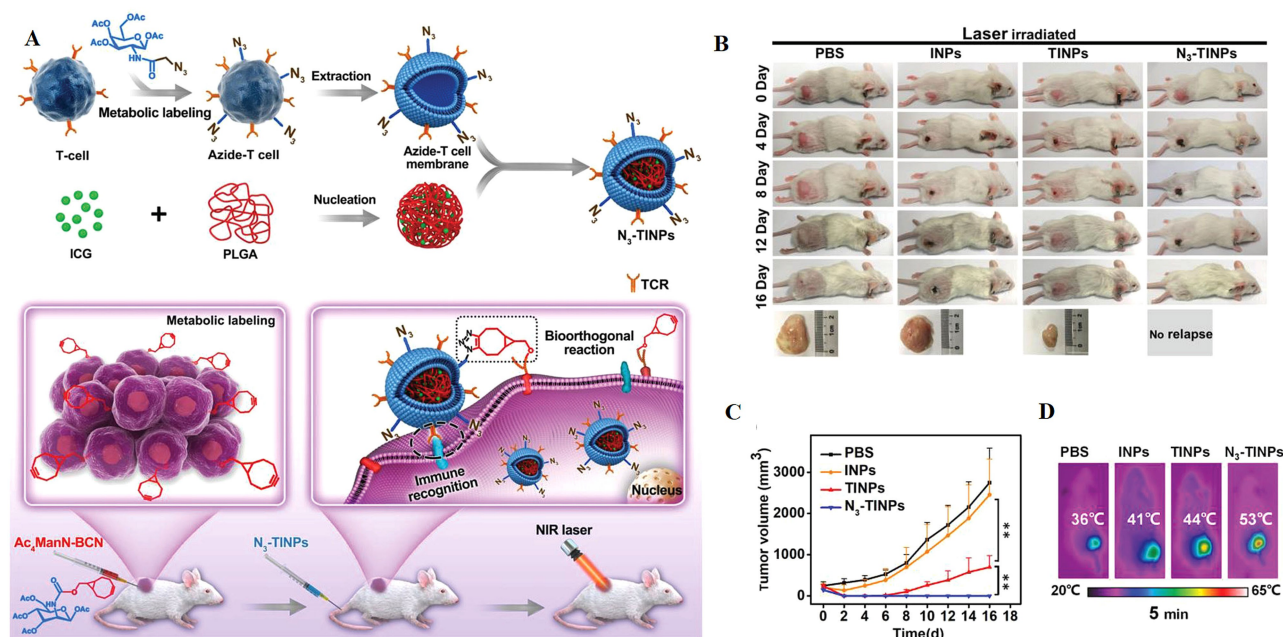


**Figure 5.** In vivo PTT by Cai et al.<sup>[73]</sup> a) Schematic illustration of dual tumor targeting. N<sub>3</sub>-TINPs are filled with ICG-PLGA polymeric cores and coated with extracted azide-tagged T cell membrane (ICG: indocyanine green, PLGA: poly(lactic-co-glycolic acid)). Tumor cells are tagged metabolically with Ac<sub>4</sub>ManN-BCN. N<sub>3</sub>-TINPs target tumor cells through immune recognition of T cell membrane and bioorthogonal SPAAC reaction between azide and BCN. b) Elimination of Raji tumor from mice models on representative photos and extracted tumors after 16-day treatment (controls: INPs: ICG loaded in PLGA-lipid nanoparticles, TINPs: ICG loaded in PLGA-T cell membrane nanoparticle); c) Raji tumor growth curves (n = 5); d) Infrared thermal images of tumor-bearing mice (laser irradiation at 808 nm) (adapted from Ref. [73] with permission. Copyright © 2019 The Authors. Published by WILEY-VCH Verlag GmbH & Co. KgaA, Weinheim).

yanine green nanoparticles (INP) with azide-labelled T cell membrane (N<sub>3</sub>-TINP) (Figure 5a). In in vitro experiments N<sub>3</sub>-TINP selectively targeted Raji tumor cells which were tagged glycometabolically with Ac<sub>4</sub>ManN-BCN. Translocated T cell membranes target tumor tissues through retained immune recognition receptors with 1.5-fold enhancement due to bioorthogonal reaction between the azide and BCN. BCN-tagged tumor-bearing mice were injected i.v. with N<sub>3</sub>-TINP, followed by laser irradiation at 808 nm. The authors noticed higher temperature increase ( $\Delta T = 17^\circ\text{C}$ ) and distinct tumor elimination with no relapse during the treatment (Figure 5b–d).

Xing et al. assembled a tumor targeting nanoagent based on zinc(II) phthalocyanine with DBCO handle (DBCO-ZnPc-LP).<sup>[74]</sup> Passive targeting of A549 tumor cells with Ac<sub>4</sub>ManNAz nanomicelles in nude mice was followed by a SPAAC labelling with DBCO-ZnPc-LP. Under 808 nm NIR light, not only could this agent produce cytotoxic heat (photothermal conversion efficiency of 44%) but it also generated an ultrasound shockwave, which resulted in cell damage (cell viability 35%) and in vivo tumor regression. Moreover, DBCO-ZnPc-LP served as a contrast agent for photoacoustic detection of tumor cells.

### 3.3. Bioorthogonally assisted photoactivated chemotherapy

Despite the several examples in bioorthogonally modulated PSs in PDT applications, bioorthogonally modified PPGs

are rare. In fact, to the best of our knowledge, the only example that employs direct activation of photoresponsivity by a bioorthogonal step was presented by our group in 2020.<sup>[75]</sup> In this example, we took advantage of the tetrazine moiety that can efficiently quench the excited states of coumarins through non-radiative pathways to allow the design of a conditionally activatable photocage that can respond to blue light following a bioorthogonal ligation step via IEDDA. We have demonstrated that the bioorthogonally applicable tetrazine motif disables the photoresponsivity of the coumarin photocage, carrying various payloads (e.g. **10**, Figure 6a). Once the tetrazine participated in a bioorthogonal ligation reaction (e.g., with BCN-functionalized mitochondria targeting triphenylphosphonium—TPP), the photocage becomes photoresponsive and cleavable by light. Such conditionally activatable photo-decaging was demonstrated in live A-431 cells using confocal microscopy through the release of a fluorogenic payload in response to a bioorthogonal reaction and light.

Contrary to the previous examples where the bioorthogonal step activated the photoresponsivity, novel approaches rather rely on the prior photoactivation of bioorthogonal functions.<sup>[1,76]</sup> Photoclick chemistry refers to a set of click reactions that are activated upon light irradiation. Combination of photoclick reactions with so-called click-to-release mechanisms could in theory result in light-assisted control of drug release via the photoactivation of bioorthogonal function.<sup>[77,78]</sup> In click-to-release reactions the prodrugs are transiently disabled by a bioorthogonal function (i.e., a

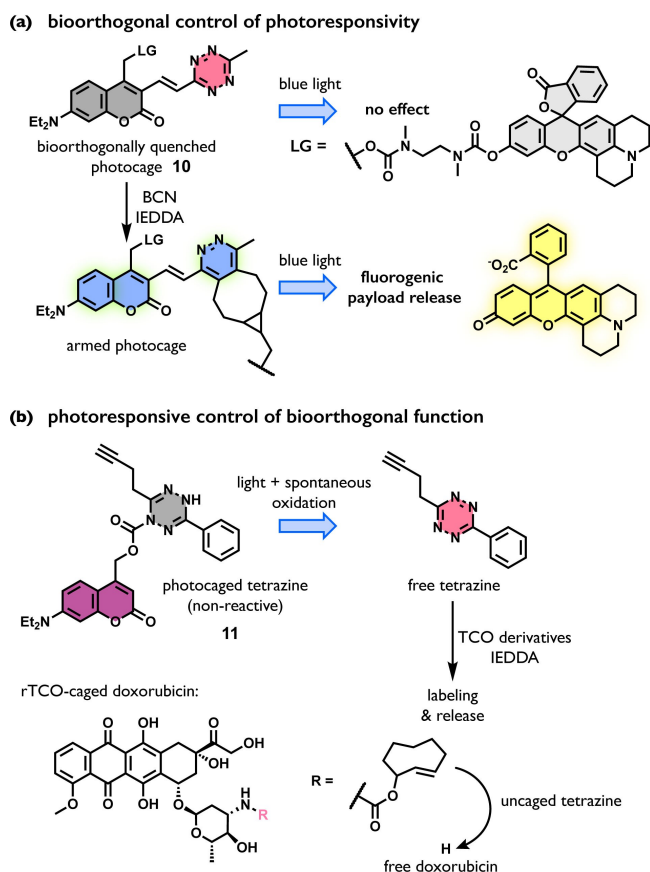


**Figure 6.** Schematic illustration of modulatable a) photoresponsivity and b) bioorthogonality.

release TCO (rTCO) or a click-to release tetrazine (crTet)).<sup>[79,80]</sup> Such bioorthogonal cleavage reactions are widely used, and already the subject of clinical trials for advanced solid tumors and non-Hodgkin lymphoma.<sup>[81,82]</sup> In a recent report, Devaraj and co-workers demonstrated light-assisted tetrazine activation from caged dihydrotetrazines (**11**, Figure 6b).<sup>[83]</sup> Photocaging prevented oxidation of dihydrotetrazine to tetrazine rendering it inactive in IEDDA reaction with dienophiles. The caging group was rapidly removed by 405 nm LED light irradiation allowing spontaneous formation of tetrazine in the cellular environment. The in situ formed tetrazine was able to react with a rTCO-caged doxorubicin. The blue light-controlled activation of cytotoxic effect on Hep 3b human liver cancer cells with an 57% loss of cell viability, which was comparable to the effects of doxorubicin alone.

In 2021, Yu et al. reported a fluorogenic photoclick-to-release system, adding a new light-controlled element to existing click-to-release strategies.<sup>[84]</sup> They demonstrated that the photoclick reaction between a monoarylsydnone and phenoxyfumarate initiated by 405 nm light irradiation leads to the formation of fluorogenic pyrazole and subsequent release of phenoxy cargo. Further to this, in 2023, Liu et al. described a cyclopropenone-caged strained alkyne precursor which was unmasked by UV light to react with

dienones with an accompanied release of carbon-monoxide followed by cancer cell cytotoxicity.<sup>[85]</sup>

### 3.4. Bioorthogonally activated combination phototherapies

In PDT, the cytotoxic effect of the PS is highly dependent on the concentration of oxygen. However, many tumors, especially solid tumors, are rather poorly vascularized therefore are hypoxic, limiting the use of PDT.<sup>[86]</sup> This serious limitation prompted the development of multimodal phototherapies assisted by bioorthogonal reactions. In 2022, Sun and co-workers detailed a multifunctional photochemotherapeutic molecule with four different synergistic functions.<sup>[87]</sup> In their design, the push-pull chromophore, 2,1,3-benzothiadiazole (BTD) a known PS and fluorescent reporter served as a core. The appending nitro group at position 5 quenches the fluorescence of BTD via PET and also serves as a nitrite-donor for bioorthogonal  $S_NAr$  reaction with dithiol-tagged  $\beta$ -galactosamine (Gal-SS). The design also included a chloropropylamine motif to effect ER targeting. The click-to-release reaction with Gal-SS led to the elimination of a TRPV1 agonist, nonivamide from position 4 and converted the quenched BTD to an efficient sensitizer of ROS. Concomitant release of  $NO_2^-$  induced the production of reactive nitrogen species, which together with the ROS resulted in serious distress in the ER.

Wu et al. combined chemo- and photothermal therapy for tumor inhibition.<sup>[88]</sup> They prepared a camptothecin-vinyl ether prodrug encapsulated within phospholipid liposomes. The chemotherapeutic can be released in a bioorthogonal bond cleavage reaction with tetrazine. An interesting work of You and co-workers presented PTT and PDT with concurrent photocatalysis, in tumor cells using heterogeneous copper nanoparticles.<sup>[89]</sup> In their setup, mesoporous carbon nanospheres doped with Cu nanoparticles induced the generation of ROS under 808 nm light with simultaneous increase in local temperature ( $\Delta T \approx 20^\circ C$ ). The authors took further advantage of the concurrent  $Cu^0 \rightarrow Cu^I$  conversion to catalyze a CuAAC reaction to assemble a resveratrol-mimetic derivative.

## 4. Summary and Outlook

The above examples aim to provide the readers with an overview of very recent developments in the field of bioorthogonally activated photoresponsivity in the context of phototherapies. Not discussed above is the fluorogenic nature of bioorthogonally activated photoresponsive species, which can be exploited in theranostic applications. These fundamental, bottom-up studies are useful to have a clear picture of the modulation strategies such bioorthogonal transformations can inflict on the photophysical properties. Often, especially in the therapeutically optimal red/NIR range, the bioorthogonal modulation effect is diminished, which either triggers smart solutions or limits the application of bioorthogonality to simple targeting. Notable smart solutions are the approaches that rely on the photocon-



trolled activation of bioorthogonal functions, such as photocaged tetrazines or recent results on photocatalytically activated tetrazines.<sup>[83,90]</sup> These are especially promising approaches in combination with drugs disabled by a cleavable complementary bioorthogonal function.

However, the significance of bioorthogonally assisted phototherapies must be carefully evaluated. The limited photo- and/or physiological stability of bioorthogonal quencher moieties i.e., the azide and the tetrazine can lead to their degradation, and consequently to the premature activation of the appending photoresponsive unit.<sup>[91–93]</sup> Complications may also arise from the need for dosing the complementary bioorthogonal function. In this respect, the stability of TCO derivatives should also be carefully evaluated.<sup>[94,95]</sup> To avoid off-target activation novel innovative chemical solutions are required. Furthermore, the difference between the photoactivated performance of the disabled and armed forms should be weighed to judge the advantages of pretargeting based ligation-dependent modulation methods over simpler preassembled constructs. For these considerations it is also important to find the right applications for bioorthogonally assisted phototherapies. Since light itself provides an excellent means of spatiotemporal control in case of non-operable, isolated tumors, one such area where bioorthogonally activated phototherapeutics are envisioned to find useful application is the treatment of diffuse/disperse tumors, especially when spread to a larger area.

To unleash the full potential of bioorthogonal chemistry assisted phototherapeutics, however, a paradigm shift is needed to switch from chemistry-driven applications to disease-based approaches. As discussed by others,<sup>[4,5,12]</sup> successful translation of novel technologies require the clear identification of the right indication—a wisely selected disease with a discernible clinical relevance. Importantly, not only should such “therapeutic argument” entail an acknowledged need for new therapies but must also be made on the basis of the enhanced selectivity of the combination of bioorthogonal chemistry and light irradiation—while also meeting the obvious physical and biological requirements of the technology (i.e., light accessibility, presence of a targetable feature etc.). Based on the success of photoimmunotherapy,<sup>[96]</sup> it is also important to mention the potential synergistic immune-enhancing effect of phototherapeutics, especially PDT, which can significantly contribute to survival through the eradication of disseminated tumor cells. Nevertheless, the understanding of the underlying chemistry and photophysics will certainly facilitate the translation of these concepts to an actual therapeutic modality as well as provide the chemical biology community with unique tools possessing remarkable selectivity.

### Acknowledgements

This work has been implemented with the support provided by the Ministry of Innovation and Technology of Hungary (NKFIH-K-143581, NKFIH-PD-135121 and VEKOP-2.3.3-15-2016-00011) M.B. and E.K. are grateful for the support of

the Hungarian Academy of Sciences (BO/00204/21 János Bolyai Research Scholarship and 140/3/2023/KP). Figures were created using Biorender.com.

### Conflict of Interest

The authors declare no conflict of interest.

### Data Availability Statement

Data sharing is not applicable to this article as no new data were created or analyzed in this study.

**Keywords:** Activatable · Bioorthogonal · Cancer · Phototherapy · Targeting

- [1] B. D. Fairbanks, L. J. Macdougall, S. Mavila, J. Sinha, B. E. Kirkpatrick, K. S. Anseth, C. N. Bowman, *Chem. Rev.* **2021**, *121*, 6915–6990.
- [2] K. Hüll, J. Morstein, D. Trauner, *Chem. Rev.* **2018**, *118*, 10710–10747.
- [3] B. Huang, H. Babcock, X. Zhuang, *Cell* **2010**, *143*, 1047–1058.
- [4] S. Monro, K. L. Colón, H. Yin, J. Roque III, P. Konda, S. Gujar, R. P. Thummel, L. Lilge, C. G. Cameron, S. A. McFarland, *Chem. Rev.* **2019**, *119*, 797–828.
- [5] B. M. Vickerman, E. M. Zywot, T. K. Tarrant, D. S. Lawrence, *Nat. Chem. Rev.* **2021**, *5*, 816–834.
- [6] A. Bansal, Y. Zhang, *Acc. Chem. Res.* **2014**, *47*, 3052–3060.
- [7] K. Ganesh, J. Massagué, *Nat. Med.* **2021**, *27*, 34–44.
- [8] B. Q. Spring, A. O. Abu-Yousif, A. Palanisami, I. Rizvi, X. Zheng, Z. Mai, S. Anbil, R. B. Sears, L. B. Mensah, R. Goldschmidt, S. S. Erdem, E. Oliva, T. Hasan, *Proc. Natl. Acad. Sci. USA* **2014**, *111*, E933–E942.
- [9] R. L. Yanovsky, D. W. Bartenstein, G. S. Rogers, S. J. Isakoff, S. T. Chen, *Photodermatol. Photoimmunol. Photomed.* **2019**, *35*, 295–303.
- [10] X. Li, J. F. Lovell, J. Yoon, X. Chen, *Nat. Rev. Clin. Oncol.* **2020**, *17*, 657–674.
- [11] H. Xiong, Y. Xu, B. Kim, H. Rha, B. Zhang, M. Li, G. F. Yang, J. S. Kim, *Chem* **2023**, *9*, 29–64.
- [12] S. Bonnet, *Dalton Trans.* **2018**, *47*, 10330–10343.
- [13] D. Wu, K. Yang, Z. Zhang, Y. Feng, L. Rao, X. Chen, G. Yu, *Chem. Soc. Rev.* **2022**, *51*, 1336–1373.
- [14] M. M. A. Mitry, F. Greco, H. M. I. Osborn, *Chem. Eur. J.* **2023**, *29*, e202203942.
- [15] S. L. Scinto, D. A. Bilodeau, R. Hincapie, W. Lee, S. S. Nguyen, M. Xu, C. W. am Ende, M. G. Finn, K. Lang, Q. Lin, J. P. Pezacki, J. A. Prescher, M. S. Robillard, J. M. Fow, *Nat. Rev. Methods Primers* **2021**, *1*, 30.
- [16] S. Kwiatkowski, B. Knap, D. Przystupski, J. Saczko, E. Kędzierska, K. Knap-Czop, J. Kotlinska, O. Michel, K. Kotowski, J. Kulbacka, *Biomed. Pharmacother.* **2018**, *106*, 1098–1107.
- [17] C. Queirós, P. M. Garrido, J. Maia Silva, P. Filipe, *Dermatol. Ther.* **2020**, *33*, e13997.
- [18] P. Agostinis, K. Berg, K. A. Cengel, T. H. Foster, A. W. Girotti, S. O. Gollnick, S. M. Hahn, M. R. Hamblin, A. Juzeniene, D. Kessel, M. Korbelik, J. Moan, P. Mroz, D. Nowis, J. Piette, B. C. Wilson, *Ca-Cancer J. Clin.* **2011**, *61*, 250–281.

- [19] P. Soergel, M. Loning, I. Staboulidou, C. Schippert, P. Hillmann, *J. Environ. Pathol. Toxicol. Oncol.* **2008**, *27*, 307–320.
- [20] T. C. Pham, V. N. Nguyen, Y. Choi, S. Lee, J. Yoon, *Chem. Rev.* **2021**, *121*, 13454–13619.
- [21] A. P. Castano, T. N. Demidova, M. R. Hamblin, *Photodiagn. Photodyn. Ther.* **2004**, *1*, 279–293.
- [22] C. Li, Y. Cheng, D. Li, Q. An, W. Zhang, Y. Zhang, Y. Fu, *Int. J. Mol. Sci.* **2022**, *23*, 7909.
- [23] J. R. Melamed, R. S. Edelman, E. S. Day, *ACS Nano* **2015**, *9*, 6–11.
- [24] S. Y. Emelianov, P.-C. Li, M. O'Donnell, *Phys. Today* **2009**, *62*, 34–39.
- [25] L. Wang, S. Hu, *Science* **2012**, *335*, 1458–1462.
- [26] C. Xu, R. Ye, H. Shen, J. W. Y. Lam, Z. Zhao, B. Z. Tang, *Angew. Chem. Int. Ed.* **2022**, *61*, e202204604.
- [27] B. Kang, D. Yu, Y. Dai, S. Chang, D. Chen, Y. Ding, *Small* **2009**, *5*, 1292–1301.
- [28] H. Yu, J. Li, D. Wu, Z. Qiu, Y. Zhang, *Chem. Soc. Rev.* **2010**, *39*, 464–473.
- [29] M. M. Dcona, J. E. Sheldon, D. Mitra, M. C. T. Hartman, *Bioorg. Med. Chem. Lett.* **2017**, *27*, 466–469.
- [30] M. Klausen, M. Blanchard-Desce, *J. Photochem. Photobiol. C* **2021**, *48*, 100423.
- [31] A. R. Sekhar, Y. Chitose, J. Janoš, S. I. Dangoor, A. Ramundo, R. Satchi-Fainaro, P. Slavíček, P. Klán, R. Weinstain, *Nat. Commun.* **2022**, *13*, 3614.
- [32] D. Castelvetti, H. Ledford, *Nature* **2022**, *610*, 242–243.
- [33] J. A. Prescher, C. R. Bertozzi, *Nat. Chem. Biol.* **2005**, *1*, 13–21.
- [34] H. Wu, S. C. Alexander, S. Jin, N. K. Devaraj, *J. Am. Chem. Soc.* **2016**, *138*, 11429–11432.
- [35] R. S. Erdmann, H. Takakura, A. D. Thompson, F. Rivera-Molina, E. S. Allgeyer, J. Beewersdorf, D. Toomre, A. Schepartz, *Angew. Chem. Int. Ed.* **2014**, *53*, 10242–10246.
- [36] A. Arsic, C. Hagemann, N. Stajkovic, T. Schubert, I. Nikic-Spiegel, *Nat. Commun.* **2022**, *13*, 314.
- [37] A. Herner, I. Nikic, M. Kállay, E. A. Lemke, P. Kele, *Org. Biomol. Chem.* **2013**, *11*, 3297–3306.
- [38] W. Mao, W. Chi, X. He, C. Wang, X. Wang, H. Yang, X. Liu, H. Wu, *Angew. Chem. Int. Ed.* **2022**, *61*, e202117386.
- [39] J. C. T. Carlson, L. G. Meimetis, S. A. Hilderbrand, R. Weisleder, *Angew. Chem. Int. Ed.* **2013**, *52*, 6917–6920.
- [40] E. Kozma, G. Estrada Girona, G. Paci, E. A. Lemke, P. Kele, *Chem. Commun.* **2017**, *53*, 6696–6699.
- [41] A. Wiczorek, P. Werther, J. Euchner, R. Wombacher, *Chem. Sci.* **2017**, *8*, 1506–1510.
- [42] P. Shieh, M. S. Siegrist, A. J. Cullen, C. R. Bertozzi, *Proc. Natl. Acad. Sci. USA* **2014**, *111*, 5456–5461.
- [43] A. Loudet, K. Burgess, *Chem. Rev.* **2007**, *107*, 4891–4932.
- [44] G. Linden, L. Zhang, F. Pieck, U. Linne, D. Kosonkov, R. Tonner, O. Vázquez, *Angew. Chem. Int. Ed.* **2019**, *58*, 12868–12873.
- [45] W. Yi, P. Xiao, X. Liu, Z. Zhao, X. Sun, J. Wang, L. Zhou, G. Wang, H. Cao, D. Wang, Y. Li, *Signal Transduction Targeted Ther.* **2022**, *7*, 386.
- [46] J. C. H. Chu, C. T. T. Wong, D. K. P. Ng, *Angew. Chem. Int. Ed.* **2023**, *62*, e202214473.
- [47] Y. Zhou, R. C. H. Wong, G. Dai, D. K. P. Ng, *Chem. Commun.* **2020**, *56*, 1078–1081.
- [48] X. Guo, R. C. H. Wong, Y. Zhou, D. K. P. Ng, P. C. Lo, *Chem. Commun.* **2019**, *55*, 13518–13521.
- [49] J. Xiong, E. Y. Xue, Q. Wu, P. C. Lo, D. K. P. Ng, *J. Controlled Release* **2023**, *353*, 663–674.
- [50] T. Y. Ohulchanskyy, D. J. Donnelly, M. R. Detty, P. N. Prasad, *J. Phys. Chem. B* **2004**, *108*, 8668–8672.
- [51] X. Chen, T. Pradhan, F. Wang, J. S. Kim, J. Yoon, *Chem. Rev.* **2012**, *112*, 1910–1956.
- [52] M. Chiba, Y. Ichikawa, M. Kamiya, T. Komatsu, T. Ueno, K. Hanaoka, T. Nagano, N. Lange, Y. Urano, *Angew. Chem. Int. Ed.* **2017**, *56*, 10418–10422.
- [53] W. Lv, S. Chi, W. Feng, T. Liang, D. Song, Z. Liu, *Chem. Commun.* **2019**, *55*, 7037–7040.
- [54] B. M. Luby, C. D. Walsh, G. Zheng, *Angew. Chem. Int. Ed.* **2019**, *58*, 2558–2569.
- [55] S. Liu, G. Feng, B. Z. Tang, B. Liu, *Chem. Sci.* **2021**, *12*, 6488–6506.
- [56] F. Hu, D. Mao, Kenry, X. Cai, W. Wu, D. Kong, B. Liu, *Angew. Chem. Int. Ed.* **2018**, *57*, 10182–10186.
- [57] Y. Yuan, S. Xu, X. Cheng, X. Cai, B. Liu, *Angew. Chem. Int. Ed.* **2016**, *55*, 6457–6461.
- [58] L. C. C. Lee, K. K. W. Lo, *J. Am. Chem. Soc.* **2022**, *144*, 14420–14440.
- [59] L. K. McKenzie, H. E. Bryant, J. A. Weinstein, *Coord. Chem. Rev.* **2019**, *379*, 2–29.
- [60] P. K. K. Leung, K. K. W. Lo, *Chem. Commun.* **2020**, *56*, 6074–6077.
- [61] L. Cheng, C. Wang, L. Feng, K. Yang, Z. Liu, *Chem. Rev.* **2014**, *114*, 10869–10939.
- [62] X. Luan, Y. Pan, Y. Gao, Y. Song, *J. Mater. Chem. B* **2021**, *9*, 7076–7099.
- [63] S. Lee, H. Koo, J. H. Na, S. J. Han, H. S. Min, S. J. Lee, S. H. Kim, S. H. Yun, S. Y. Jeong, I. C. Kwon, K. Choi, K. Kim, *ACS Nano* **2014**, *8*, 2048–2063.
- [64] Y. Nakamura, A. Mochida, P. L. Choyke, H. Kobayashi, *Bioconjugate Chem.* **2016**, *27*, 2225–2238.
- [65] L. Taiariol, C. Chaix, C. Farre, E. Moreau, *Chem. Rev.* **2022**, *122*, 340–384.
- [66] S. Pandit, D. Dutta, S. Nie, *Nat. Mater.* **2020**, *19*, 478–480.
- [67] J. Wu, *J. Pers. Med.* **2021**, *11*, 771.
- [68] R. Wie, Y. Dong, Y. Tu, S. Luo, X. Pang, W. Zhang, W. Yao, W. Tang, H. Yang, X. Wei, X. Jiang, Y. Yuan, R. Yang, *ACS Appl. Mater. Interfaces* **2021**, *13*, 14004–14014.
- [69] Z. Cao, D. Li, L. Zhao, M. Liu, P. Ma, Y. Luo, X. Yang, *Nat. Commun.* **2022**, *13*, 2038.
- [70] J. Gao, B. Hou, Q. Zhu, L. Yang, X. Jiang, Z. Zou, X. Li, T. Xu, M. Zheng, Y. H. Chen, Z. Xu, H. Xu, H. Yu, *Nat. Commun.* **2022**, *13*, 4318.
- [71] J. Qiao, F. Tian, Y. Deng, Y. Shang, S. Chen, E. Chang, J. Yao, *Theranostics* **2020**, *10*, 5305–5321.
- [72] W. Zhang, W. Deng, H. Zhang, X. Sun, T. Huang, W. Wang, P. Sun, Q. Fan, W. Huang, *Biomaterials* **2020**, *243*, 119934.
- [73] Y. Han, H. Pan, W. Li, Z. Chen, A. Ma, T. Yin, R. Liang, F. Chen, Y. Ma, Y. Jin, M. Zheng, B. Li, L. Cai, *Adv. Sci.* **2019**, *6*, 1900251.
- [74] L. Du, H. Qin, T. Ma, T. Zhang, D. Xing, *ACS Nano* **2017**, *11*, 8930–8943.
- [75] M. Bojtár, K. Németh, F. Domahidy, G. Knorr, A. Verkman, M. Kállay, P. Kele, *J. Am. Chem. Soc.* **2020**, *142*, 15164–15171.
- [76] G. S. Kumar, Q. Lin, *Chem. Rev.* **2021**, *121*, 6991–7031.
- [77] X. Ji, Z. Pan, B. Yu, L. K. de La Cruz, Y. Zheng, B. Ke, B. Wang, *Chem. Soc. Rev.* **2019**, *48*, 1077–1094.
- [78] J. Wang, X. Wang, X. Fan, P. R. Chen, *ACS Cent. Sci.* **2021**, *7*, 929–943.
- [79] R. Rossin, S. M. J. van Duijnhoven, W. ten Hoeve, H. M. Janssen, L. H. J. Kleijn, F. J. M. Hoeven, R. M. Versteegen, M. S. Robillard, *Bioconjugate Chem.* **2016**, *27*, 1697–1706.
- [80] A. H. A. M. van Onzen, R. M. Versteegen, F. J. M. Hoeven, I. A. W. Pilot, R. Rossin, T. Zhu, J. Wu, P. J. Hudson, H. M. Janssen, W. Hoeve, M. S. Robillard, *J. Am. Chem. Soc.* **2020**, *142*, 10955–10963.
- [81] ClinicalTrials.gov Identifier: NCT04106492.
- [82] ClinicalTrials.gov Identifier: NCT03682796.
- [83] L. Liu, D. Zhang, M. Johnson, N. K. Devaraj, *Nat. Chem.* **2022**, *14*, 1078–1085.

- [84] H. Liu, T. Zheng, Y. Zheng, B. Li, X. Xie, X. Shen, X. Zhao, Z. Yu, *Chem. Commun.* **2021**, 57, 8135–8138.
- [85] M. Liu, Y. Wang, Z. Yan, J. Yang, Y. Wu, D. Ding, X. Ji, *ChemBioChem* **2022**, 23, e202200506.
- [86] M. Höckel, P. Vaupel, *JNCI J. Natl. Cancer Inst.* **2001**, 93, 266–276.
- [87] J. Sun, X. Zhang, X. Wang, J. Peng, G. Song, Y. Di, F. Feng, S. Wang, *Angew. Chem. Int. Ed.* **2022**, 61, e202213765.
- [88] X. Xie, B. Li, J. Wang, C. Zhan, Y. Huang, F. Zeng, S. Wu, *ACS Appl. Mater. Interfaces* **2019**, 11, 41875–41888.
- [89] Y. You, F. Cao, Y. Zhao, Q. Deng, Y. Sang, Y. Li, K. Dong, J. Ren, X. Qu, *ACS Nano* **2020**, 14, 4178–4187.
- [90] A. Jemas, Y. Xie, J. E. Pigga, J. L. Caplan, C. W. am Ende, J. M. Fox, *J. Am. Chem. Soc.* **2022**, 144, 1647–1662.
- [91] M. R. Karver, R. Weissleder, S. A. Hildebrand, *Bioconjugate Chem.* **2011**, 22, 2263–2270.
- [92] A. B. Neef, N. W. Luedtke, *ChemBioChem* **2014**, 15, 789–793.
- [93] E. P. Kyba, R. A. Abramovitch, *J. Am. Chem. Soc.* **1980**, 102, 735–740.
- [94] J. M. J. M. Ravasco, J. A. S. Coelho, A. F. Trindade, C. A. M. Alfonso, *Pure Appl. Chem.* **2020**, 92, 15–23.
- [95] J. E. Hoffmann, T. Plass, I. Nikic, I. V. Aramburu, C. Koehler, H. Gillandt, E. A. Lemke, C. Schultz, *Chem. Eur. J.* **2015**, 21, 12266–12270.
- [96] T. Kato, H. Wakiyama, A. Furusawa, P. L. Choyke, H. Kobayashi, *Cancers* **2021**, 13, 2535.

Manuscript received: March 3, 2023

Accepted manuscript online: May 10, 2023

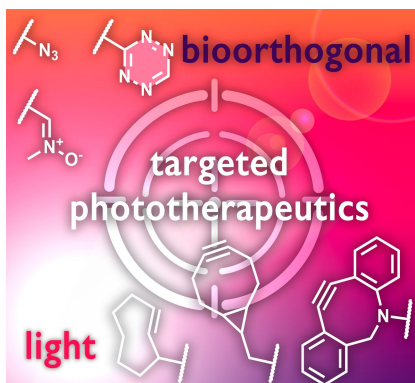
Version of record online: ■■, ■■

## Minireviews

## Photochemistry

E. Kozma, M. Bojtár,  
P. Kele\* \_\_\_\_\_ e202303198

Bioorthogonally Assisted Phototherapy: Recent Advances and Prospects



Phototherapeutic approaches combined with bioorthogonal chemistry are expected to significantly improve the spatiotemporal precision of targeted therapies. As a result, related bioorthogonally assisted phototherapy research has recently intensified. This minireview briefly discusses the latest developments in the state of the art.